Transfer-matrix density-matrix renormalization group for stochastic models: the Domany-Kinzel cellular automaton

2001 J. Phys. A: Math. Gen. 34 L279

(http://iopscience.iop.org/0305-4470/34/19/103)

INSTITUTE OF PHYSICS PUBLISHING JOURNAL OF PHYSICS A: MATHEMATICAL AND GENERAL

J. Phys. A: Math. Gen. **34** (2001) L279–L287 www.iop.org/Journals/ja PII: S0305-4470(01)23309-5

LETTER TO THE EDITOR

Transfer-matrix density-matrix renormalization group for stochastic models: the Domany–Kinzel cellular automaton*

A Kemper, A Schadschneider and J Zittartz

Institut für Theoretische Physik, Universität zu Köln, Zülpicher Strasse 77, D-50937 Köln, Germany

E-mail: kemper@thp.uni-koeln.de and as@thp.uni-koeln.de

Received 21 March 2001

Abstract

We apply the transfer-matrix density-matrix renormalization group (TMRG) to a stochastic model, the Domany–Kinzel cellular automaton, which exhibits a non-equilibrium phase transition in the directed percolation universality class. Estimates for the stochastic time evolution, phase boundaries and critical exponents can be obtained with high precision. This is possible using only modest numerical effort since the thermodynamic limit can be taken analytically in our approach. We also point out further advantages of the TMRG over other numerical approaches, such as classical DMRG or Monte Carlo simulations.

PACS numbers: 0250E, 6460H, 0270, 0510C, 0565

1. Introduction

The density-matrix renormalization group (DMRG) is a powerful numerical tool, which was developed by White [1, 2] to investigate one-dimensional quantum chains. Since then it has been applied to several problems in quantum and classical physics [3].

DMRG studies of one-dimensional stochastic processes represent a relatively new field of interest. Such models can be described in terms of a non-symmetric stochastic Hamiltonian H [4,5]. The treatment of non-symmetric matrices within a DMRG algorithm [6–8] is a more challenging task than that of quantum systems. Carlon *et al* [8] have systematically studied the application of the 'classical' DMRG to reaction–diffusion models. They showed that it is possible to obtain accurate results for non-equilibrium phase transitions and their critical properties.

We propose here a different DMRG approach to study stochastic models, namely the transfer-matrix DMRG (TMRG). This method was first applied to two-dimensional classical systems by Nishino [9]. Xiang *et al* [10,11] used the TMRG to investigate the quantum transfer

* Dedicated to Professor Erwin Müller-Hartmann on the occasion of his 60th birthday.

0305-4470/01/190279+09$30.00

matrix of one-dimensional quantum systems and introduced an accurate method for studying thermodynamic properties [12].

As an example we choose the Domany–Kinzel cellular automaton (DKCA) [13,14], which exhibits a non-equilibrium phase transition in the universality class of directed percolation (DP) [14, 15]. Its phase diagram and critical properties are well known from previous studies (cf [16] for a review). We compare these literature data to our TMRG results to demonstrate their accuracy. Important advantages of our approach over DMRG and Monte Carlo simulations (MCSs) are pointed out, especially for systems such as the DKCA for which the infinite-time limit ($t \to \infty$) and the thermodynamic limit ($N \to \infty$) do not commute.

2. The Domany–Kinzel cellular automaton

Cellular automata are algorithms that map one discrete configuration of a lattice to a new one in discrete time steps. Usually the map can be decomposed into local update rules. In the following we introduce the DKCA, which is an example of a stochastic cellular automaton.

2.1. The model

The DKCA [13,14] is defined on a periodically closed chain of N sites. Each site s_i can take the values $s_i \in \{0, 1\}$. A configuration of the chain can be interpreted as a vector $|s\rangle = |s_1, \ldots, s_N\rangle$ in a 'Hilbert space'. We speak of dead ($s_i = 0$) and active ($s_i = 1$) sites. The local update rules of a site $s_i(t + 1)$ are given by certain conditional transition probabilities

$$p(s_i(t + 1)|s_{i-1}(t)s_{i+1}(t)) \tag{1}$$

which depend only on the neighbouring sites $s_{i\pm1}(t)$. The model is controlled by three independent parameters

$$p_0 := p(1|00) \qquad p_1 := p(1|01) = p(1|10) \qquad \text{and} \qquad p_2 := p(1|11) \tag{2}$$

where $p(0|\cdot) = 1 - p(1|\cdot)$. The DKCA is defined by $p_0 = 0$. We are interested in the time evolution of an initial probability distribution $P(t = 0)$ of lattice states. The phases of the model are characterized by the properties of the stationary distribution $P(t = \infty)$. The probability distribution $P(t)$ can be regarded as a vector $|P(t)\rangle = \sum_s P_s(t)\,|s\rangle$, where $P_s(t)$ denotes the probability of a state $|s\rangle$ at time step t.

2.2. Phases and critical phenomena

The phase diagram differs depending on whether we consider a finite or infinite chain length N. For a finite system only one phase occurs for arbitrary $p_1, p_2 < 1$. Any initial state $|P(0)\rangle$ decays exponentially fast to the stationary state $|0\rangle := |00\cdots0\rangle$ which consists of dead sites only. $|0\rangle$ is referred to as an *absorbing state* of the model because the system cannot escape from $|0\rangle$ due to $p_0 = 0$. However, the situation changes in the thermodynamic limit $N \to \infty$. For sufficiently large p_1 and p_2 an arbitrary initial state $|P(0)\rangle \neq |0\rangle$ evolves into an unique stationary state $|P(\infty)\rangle \neq |0\rangle$. Thus we observe two phases, an *absorbing* and an *active* one, separated by a sharp transition which falls into the DP universality class.

Consider an arbitrary curve $f(p)$ $(0 < p < 1)$ in the phase diagram (p_1, p_2), crossing the transition curve at $p = p_c$. An order parameter for the transition from the active to the absorbing phase is given by the local density of active sites

$$n_p(t) := \langle 1|\, n_i\, |P(t)\rangle \tag{3}$$

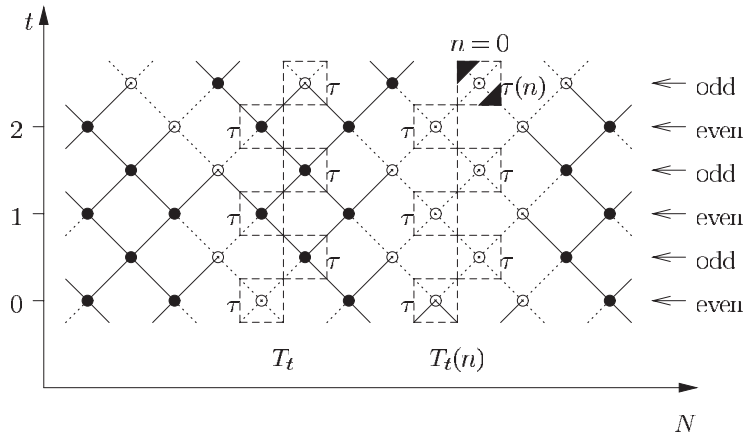

Figure 1. Sub-lattice parallel update of the DKCA.

with $|1\rangle := \sum_s |s\rangle$ and the local number operator n_i. In the absorbing phase $n_p(t)$ vanishes in the limit $t \to \infty$, while in the active phase $n_p(t)$ saturates at some stationary value $n_p(\infty)$. Close to the phase transition point p_c a power law behaviour

$$n_p(\infty) \sim (p - p_c)^{\beta} \tag{4}$$

is observed. In contrast to equilibrium systems without dynamical aspects, critical phenomena in non-equilibrium systems are usually characterized by two correlation lengths $\xi_\perp$, $\xi_\parallel$ in space and time respectively. Close to a phase transition point these correlation lengths diverge as

$$\xi_\perp \sim (p - p_c)^{-\nu_\perp} \qquad \xi_\parallel \sim (p - p_c)^{-\nu_\parallel}. \tag{5}$$

The DP universality class is already determined by the triple $(\beta, \nu_\perp, \nu_\parallel)$ [16]. Two other critical exponents α and σ are used in this work. Choosing $p \approx p_c$, the dynamic evolution of $n_p(t)$ scales as

$$n_p(t) \sim t^{-\alpha} \tag{6}$$

and the response of $n_p(\infty)$ to an 'external field' p_0 as

$$n_{p,p_0}(\infty) \sim (p_0)^{\beta/\sigma}. \tag{7}$$

α and σ can be related to β, $\nu_\perp$ and $\nu_\parallel$ using scaling theory [16]:

$$\alpha = \frac{\beta}{\nu_\parallel} \qquad \text{and} \qquad \sigma = \nu_\parallel + \nu_\perp - \beta. \tag{8}$$

3. Transfer-matrix DMRG

We first map the DKCA onto a two-dimensional classical system which can be solved using a transfer-matrix formulation. In the thermodynamic limit $N \to \infty$ the properties of the model can be inferred from the knowledge of certain eigenvalues and eigenvectors of the transfer matrix. The TMRG algorithm calculates this dominant part of the spectrum.

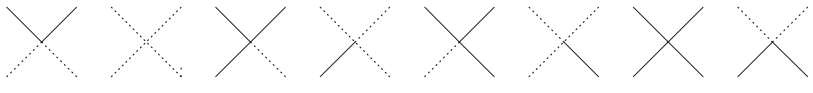

Figure 2. Vertices of the classical model with corresponding probabilities. Full lines correspond to bonds.

3.1. Mapping

The local update probabilities (1) of a site $s_i(t+1)$ only depend on the neighbouring sites $s_{i\pm1}(t)$. Hence, we use a sub-lattice (parallel) update. An update time step $t \to t+1$ is divided into two sub-steps updating the sub-lattice of odd and even sites separately. Figure 1 depicts a realization of the update. The sites are connected by two state bonds. A bond is present (full line) if the predecessor $s_{i\pm1}(t)$ of a site $s_i(t+1)$ is active, or not present (dotted line) otherwise. As shown in figure 1, the bonds form a two-dimensional square lattice Γ. A configuration $\gamma \in \Gamma$ of the lattice decomposes into vertices ν which can be in eight different states. These are shown in figure 2 together with the probabilities assigned to them.

Various properties of the stochastic system can now be expressed in terms of the statistical mechanics of a two-dimensional vertex model. To determine the critical behaviour we are mainly interested in the order parameter

$$n_p(t) = \frac{\sum_{\gamma\in\Gamma} n(\gamma)\, p(\gamma)}{\sum_{\gamma\in\Gamma} p(\gamma)}. \tag{9}$$

$p(\gamma) = \prod_{\nu\in\gamma} \nu$ denotes the probability of a certain lattice configuration γ and corresponds to the statistical weight in a vertex model. $n(\gamma) \in \{0, 1\}$ measures the state of a certain lattice site (cf figure 1). Thus the calculation of $n_p(t)$ requires taking the average $\langle n\rangle$ of a local operator n in a vertex model. Note that we have periodic boundary conditions in space direction N, but open ones in time direction t.

3.2. Transfer-matrix formulation

We briefly recall some basic facts of the transfer-matrix formulation of two-dimensional classical systems. The idea is to transform the sum over all configurations in (9) into a product of transfer matrices. The vertex model representing the dynamics of the DKCA has a checkerboard-like structure (cf figure 1). Each dashed square tags a vertex and defines a local transfer matrix

$$\tau = \left(\langle\sigma_1\sigma_2|\ \tau\ \left|\sigma_1'\sigma_2'\right\rangle\right) = \begin{array}{ccc} \sigma_2 & & \sigma_2' \\ & \times & \\ \sigma_1 & & \sigma_1' \end{array} = \begin{pmatrix} 1-p_0 & 0 & 1-p_1 & 0 \\ 0 & p_0 & 0 & p_1 \\ 1-p_1 & 0 & 1-p_2 & 0 \\ 0 & p_1 & 0 & p_2 \end{pmatrix}. \tag{10}$$

The (vertical) transfer matrix T_t is defined by the matrix elements

$$\langle\sigma_2\cdots\sigma_{2t}|\ T_t\ \left|\sigma_2'\cdots\sigma_{2t}'\right\rangle = \sum_{\substack{\{\tilde\sigma_k\}\\ \sigma_1\sigma_{2t+1}'}} \prod_{k=1}^{t} \langle\sigma_{2k-1}\sigma_{2k}|\ \tau\ |\tilde\sigma_{2k-1}\tilde\sigma_{2k}\rangle\ \langle\tilde\sigma_{2k}\tilde\sigma_{2k+1}|\ \tau\ \left|\sigma_{2k}'\sigma_{2k+1}'\right\rangle. \tag{11}$$

In (11) the open boundary conditions in the t-direction are considered by summing out σ_1, $\tilde\sigma_1$, σ_{2t+1}' and $\tilde\sigma_{2t+1}$. Note that this definition is similar to the so-called quantum transfer matrix used in [10–12] for quantum systems. In contrast to the horizontal transfer matrix in the N-direction, T_t is not a stochastic matrix.

For the calculation of the order parameter another matrix $T_t(n)$ is needed, which contains one modified local transfer matrix (see figure 1)

$$\tau(n) = \begin{pmatrix} 0 & 0 & 0 & 0 \\ 0 & p_0 & 0 & p_1 \\ 0 & 0 & 0 & 0 \\ 0 & p_1 & 0 & p_2 \end{pmatrix}. \tag{12}$$

Using T_t and $T_t(n)$ it can be easily shown that

$$n_p(t) = \frac{\operatorname{tr}\left(T_t(n) T_t^{N/2-1}\right)}{\operatorname{tr}\left(T_t^{N/2}\right)}. \tag{13}$$

Under the assumption that the highest eigenvalue Λ_0 of T_t is not degenerate, the thermodynamic limit $N \to \infty$ can be performed exactly

$$n_p(t) = \frac{\operatorname{tr}\left(T_t(n) T_t^{N/2-1}\right)}{\operatorname{tr}\left(T_t^{N/2}\right)} \xrightarrow{N\to\infty} \frac{\left\langle \Lambda_0^L \right| T_t(n) \left| \Lambda_0^R \right\rangle}{\Lambda_0} \tag{14}$$

$\left|\Lambda_0^R\right\rangle$ ($\left|\Lambda_0^L\right\rangle$) denotes the right (left) eigenvector of the non-symmetric transfer matrix T_t corresponding to the eigenvalue Λ_0.

3.3. TMRG algorithm

The TMRG calculates Λ_0 and the corresponding left and right eigenvector for an arbitrary matrix size t. This is done iteratively by numerical renormalization techniques. We do not go into the details of the algorithm, which is basically the same as used for the quantum transfer matrix in [11]. Two important modifications are necessary:

- Open boundary conditions in time direction t are used in (11). These are necessary as the DKCA is not translationally invariant in time. In contrast, the corresponding Trotter dimension in the quantum TMRG is periodically closed [11].
- The density matrix $\rho_{\mathrm{ns}} = \operatorname{tr}_{\mathrm{e}} \left|\Lambda_0^R\right\rangle\left\langle\Lambda_0^L\right|$ used in the quantum TMRG is not symmetric, where $\operatorname{tr}_{\mathrm{e}}$ denotes the partial trace over the environmental block. Following [8] we restricted ourselves to the symmetric density matrix

$$\rho_{\mathrm{s}} = \tfrac{1}{2} \operatorname{tr}_{\mathrm{e}} \left(\left|\Lambda_0^R\right\rangle\left\langle\Lambda_0^R\right| + \left|\Lambda_0^L\right\rangle\left\langle\Lambda_0^L\right| \right). \tag{15}$$

The eigenvectors $\left|\Lambda_0^R\right\rangle$ and $\left|\Lambda_0^L\right\rangle$ of T_t were calculated by a power method. The diagonalization of the density matrix was done by using MAPLE, which can in principle handle arbitrary numerical precision. The data presented in the following section have been obtained by keeping $m = 24$ states.

4. Results

4.1. Phase diagram

In the absorbing phase $n_p(t)$ decreases exponentially fast to zero, whereas $n_p(\infty) \neq 0$ in the active phase. At the transition point $p = p_c$ we expect a power law behaviour. Figure 3 (left) presents a double-logarithmic plot of n_p along a curve $f(p)$ in the phase diagram (p_1, p_2). As an example we used the site-directed percolation (SDP) line $f_{\mathrm{SDP}}(p) = (p, p)$. p_c is determined by adjusting p until the curvature of $n_p(t)$ in the double-logarithmic plot vanishes. This was done for various lines $f_{p_2}(p) = (p, p_2)$ to calculate the complete transition line (cf figure 3 (right)).

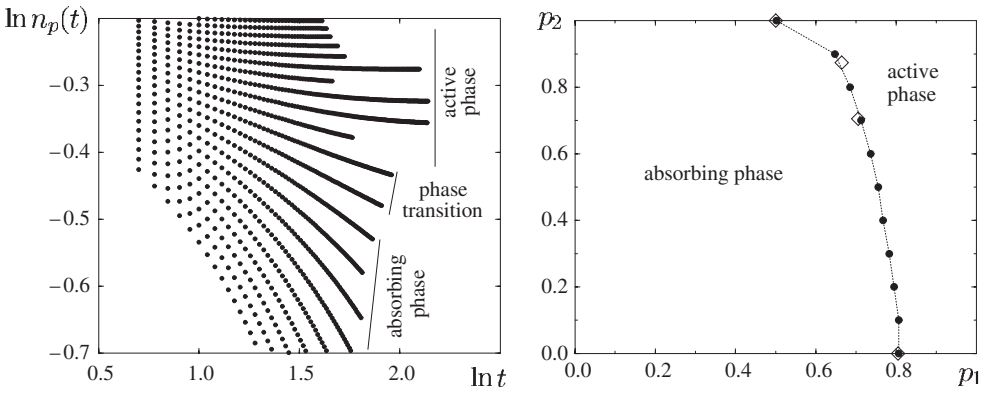

Figure 3. The left-hand panel shows the dynamic evolution of $n_p(t)$ for different p on the SDP line. The curvature of the log/log plot determines whether p belongs to the active or absorbing phase. The right-hand panel depicts the phase diagram calculated using TMRG (•) in comparison with data (◇) from [15, 17–19].

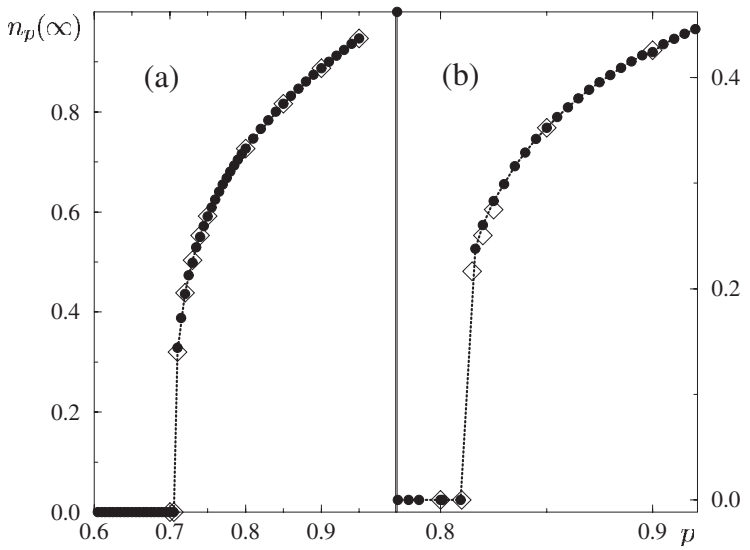

Figure 4. TMRG results (•) of $n_p(\infty)$ obtained from calculations across (*a*) the SDP line and (*b*) the line $f_0(p) = (p, 0)$. MCS data (◇) are plotted for comparison.

4.2. Order parameter

In a second step we estimated $n_p(\infty)$ in the active phase by a $1/t$ finite-size scaling. Figure 4 depicts the results we obtained for the SDP line and the line $f_0(p) = (p, 0)$. Within the phases our data are in excellent agreement with MCS. Only close to the critical point do we observe a small deviation. Here the $1/t$-scaling becomes less accurate due to critical slowing down. We expect that other methods, i.e. VBS or BST [20, 21], provide better results.

Table 1. Estimates for the critical exponents obtained by series expansion and MCS in comparison with TMRG. Results for $\nu_\parallel$ and $\nu_\perp$ can be obtained for our data using the scaling relations (8).

Critical exponent	Series [22]	MCS [23, 24]	TMRG (this work)
β	0.276 486(8)	0.276 49(4)	0.276(5)
$\nu_\parallel$	1.733 847(6)	1.733 83(3)	
$\nu_\perp$	1.096 854(4)	1.096 84(1)	
α	0.159 464(5)	0.159 46(2)	0.156(5)
β/σ	0.108 25(2)	0.108 25(2)	0.108(5)

4.3. Critical exponents

The critical exponents α, β and σ determine the universality class (cf section 2.2). We exemplify the calculation of the exponents by investigating the SDP line. Figure 5 depicts for the order parameter (*a*) its time dependence $n_p(t)$, (*b*) the stationary value $n_p(\infty)$ and (*c*) the stationary value $n_{p,p_0}(\infty)$ in the presence of a 'field' $p_0 \neq 0$ with p close to p_c. The linear regression slope of a double-logarithmic plot (see insets) yields the particular exponent. Table 1 compares the results with other data obtained by series expansion and MCS. The accuracy of the exponents is similar to the DMRG calculations performed by Carlon *et al* [8].

5. Conclusions and outlook

In this letter we have proposed a new approach to stochastic models using TMRG. The accuracy of the results was shown by comparison to MCS or literature data. Critical exponents were estimated which deviate from the currently accepted values [22] by less than 3%. In the following we focus on three important advantages of TMRG compared to traditional MCS or DMRG calculations.

First, the exact treatment of the thermodynamic limit of the chain is the main aspect of the TMRG presented here. In contrast, MCS and DMRG can only be applied to finite chains. Thus a finite-size scaling has to be used carefully to estimate the thermodynamic limit $N \to \infty$. For transitions into absorbing states $N \to \infty$ does usually not commute with the infinite-time limit $t \to \infty$. As shown in (14), $N \to \infty$ can be performed exactly within the transfer-matrix formulation.

Second, the TMRG approach facilitates a proper investigation of the dynamic evolution of the system (i.e. $n_p(t)$). This is a more difficult task using MCS. Many samples have to be taken into account to obtain a reasonable average. In contrast, the DMRG and TMRG approaches do not require random numbers and averaging as the MCS does. The DMRG algorithm basically calculates the ground state of the stochastic Hamiltonian H, which corresponds to the steady state ($t \to \infty$) [8]. Dynamic properties are available by analysing the gap of H. Thus the second eigenvalue of H has to be computed. Critical properties are then extracted from the finite-size data of the gap [8]. On the other hand, the TMRG offers direct access to the dynamics and phase transition of the model by calculating one eigenvalue only.

The third advantage is a rather technical one. We obtained surprisingly accurate results by modest numerical efforts. In comparison, the classical DMRG algorithm needs more sophisticated numerical techniques to guarantee a sufficient convergence [8]. We expect a further improvement of our results by involving various numerical refinements, i.e. a modified Arnoldi method [25] or a BST finite-size scaling [20, 21].

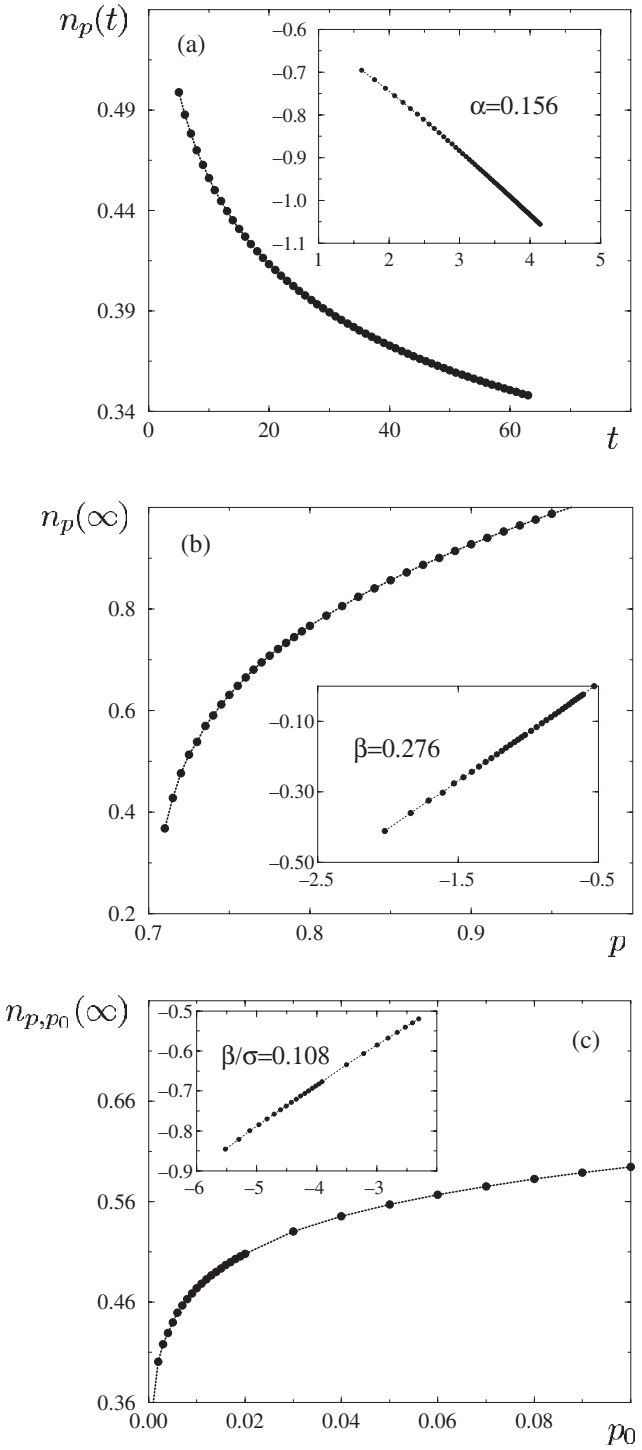

Figure 5. Calculation of the critical exponents (*a*) α, (*b*) β and (*c*) $\frac{\beta}{\sigma}$. The insets are double-logarithmic plots of the particular data. The critical exponents are calculated by determining the linear regression slope of the log/log plot.

The TMRG approach can be generalized to study other stochastic processes with arbitrary dynamics. Currently we investigate the pair contact process with diffusion (PCPD) and compare TMRG and DMRG results [26]. The universality class of the model is still unknown and an interesting field of research [27, 28].

The authors have benefited from intensive discussions with R Raupach, who placed his TMRG program for quantum systems at our disposal. We also thank M Henkel and U Schollwöck for very interesting suggestions and discussions about numerical aspects. AK thanks J Sirker for very useful discussions about the TMRG algorithm. This work was supported by SFB 341.

References

[1] White S R 1992 *Phys. Rev. Lett.* **69** 2863
[2] White S R 1993 *Phys. Rev.* B **48** 10345
[3] Peschel I, Wang X, Kaulke M and Hallberg K (ed) 1998 *Lecture Notes in Physics* vol 528 (Berlin: Springer)
[4] Alcaraz F C, Droz M, Henkel M and Rittenberg V 1994 *Ann. Phys., NY* **230** 250
[5] Schütz G 2000 *Phase Transitions and Critical Phenomena* vol 19, ed C Domb and J Lebowitz (London: Academic)
[6] Kaulke M and Peschel I 1998 *Eur. Phys. J.* B **5** 727
[7] Hieida Y 1998 *J. Phys. Soc. Japan* **67** 369
[8] Carlon E, Henkel M and Schollwöck U 1999 *Eur. Phys. J.* B **12** 99
[9] Nishino T 1995 *J. Phys. Soc. Japan* **64** 3598
[10] Bursill R J, Xiang T and Gehring G A 1996 *J. Phys.: Condens. Matter* **8** L583
[11] Wang X and Xiang T 1997 *Phys. Rev.* B **56** 5061
[12] Klümper A, Raupach R and Schönfeld F 1999 *Phys. Rev.* B **59** 3612
[13] Domany E and Kinzel W 1984 *Phys. Rev. Lett.* **53** 311
[14] Kinzel W 1985 *Z. Phys.* **58** 229
[15] Kinzel W 1983 *Annals of the Israel Physical Society* vol 5 (Bristol: Hilger)
[16] Hinrichsen H 2000 *Adv. Phys.* **49** 815
[17] Rieger H, Schadschneider A and Schreckenberg M 1994 *J. Phys. A: Math. Gen.* **27** L423
[18] Tretyakov A Y and Inui N 1995 *J. Phys. A: Math. Gen.* **28** 3985
[19] Jensen I 1996 *Phys. Rev. Lett.* **77** 4988
[20] Burlisch R and Stoer J 1964 *Numer. Math.* **6** 413
[21] Henkel M and Schütz G 1988 *J. Phys. A: Math. Gen.* **21** 2617
[22] Jensen I 1999 *J. Phys. A: Math. Gen.* **32** 5233
[23] Lauritsen K B, Sneppen K, Markosová M and Jensen M H 1997 *Physica* A **246** 1
[24] Munõs M A, Dickmann R, Vespignani A and Zapperi S 1999 *Phys. Rev.* E **59** 6175
[25] Henkel M and Schollwöck U 2000 Private communications
[26] Henkel M, Kemper A, Schadschneider A, Schollwöck U and Zittartz J 2001 work in progress
[27] Carlon E, Henkel M and Schollwöck U 2001 *Phys. Rev.* E **63** 036101
(Carlon E, Henkel M and Schollwöck U 1999 *Preprint* cond-mat/9912347)
[28] Hinrichsen H 2001 *Phys. Rev.* E **63** 036102
(Hinrichsen H 2000 *Preprint* cond-mat/0001177)